Determination of the Power Balance for Thin Ag-SnO2 Electrodes Submitted to an Electric Arc Based on IR Thermography

Romaric Landfried, Mohamed Boukhlifa, Frédéric Houzé, Thierry Leblanc, Philippe Teste

Determination of the Power Balance for Thin Ag-SnO_2 Electrodes Submitted to an Electric Arc Based on IR Thermography

R. Landfried, M. Boukhlifa, F. Houzé, T. Leblanc, Ph. Testé

GeePs | Group of electrical engineering - Paris, CNRS, CentraleSupélec, Université Paris-Saclay, Sorbonne Université, 3 & 11 rue Joliot-Curie, Plateau de Moulon 91192 Gif-sur-Yvette CEDEX, France
romaric.landfried@centralesupelec.fr

Abstract—The objective of the work presented here is to estimate the characteristics of the power balance, i.e. the power and the surface power density that the electric arc brings to Ag-SnO_2 electrodes. This work is first based on an experimental study carried out using an IR camera with which we measured the temperature in a zone close to the area impacted by the arc, but not flashed by it. In a second step, the temperature distributions obtained are compared with the results of a numerical model of the electrode heating. The model input parameters are the power *P* and the surface power density *Q*. Solving this inverse problem thus makes it possible to estimate values of *P* and *Q* leading to measured and calculated heating (temperature distribution) that are as similar as possible. Such a method has been applied for Ag-SnO_2 cathodes and anodes and for various intensities of the arc current in a range 80 - 200 A.

***Index Terms*—Circuit breakers, contactors, silver tin oxide, switches**

I. Introduction

A. Context

TODAY Ag-SnO_2 is a commonly used contact material in many components such as household switches, light switches, domestic and industrial circuit breakers, contactors and relays. During their lifetime, all these components are activated thousands of times (even hundreds of thousands). Therefore the study of the degradation of contact pads over the closing opening cycles is of great interest to switchgear manufacturers. Over the course of the tests, due to repeated heating under the action of opening or closing electric arcs, various physical phenomena contribute to the deterioration of the properties of the contact pads. In the case of Ag-SnO_2 pads for instance, mass losses of course occur, but also the appearance of cracks and of demixing zones in the material... Some contribute to the deterioration of contact resistance or to the progressive destruction of the pad and others greatly increase the risk of welding. For instance, Figure 1 [1] shows the microstructure observed with an optical microscope in the cross section of an Ag-SnO_2 electrode after 50,000 arcs (300 A rms). Bubbles and cracks can be observed in the material as a result of melting-resolidification cycles of the pseudo-metal, as well as demixing areas between silver and tin oxide.

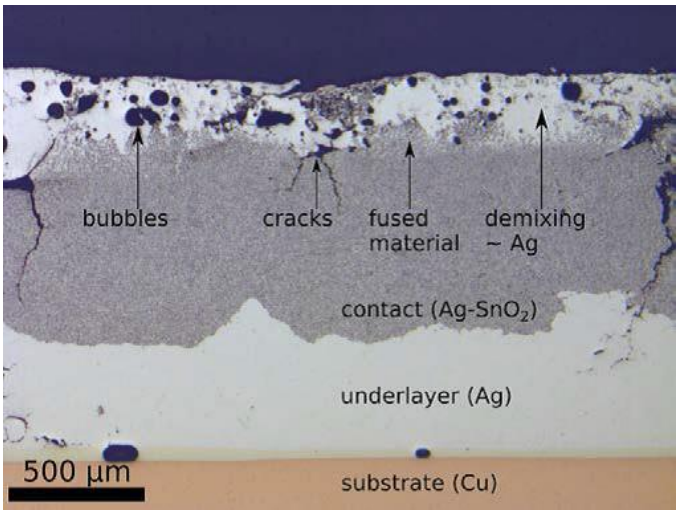

Fig. 1. Microstructure of an Ag-SnO_2 electrode after 50,000 arcs (300 A rms) observed in cross section with an optical microscope (from ref [1]).

For many years, numerous experimental works have been conducted concerning the degradation of contacts in Ag-SnO_2. Some of them propose qualitative work carried out, for example, with the help of optical observations on evaluation of changes in contact surface profiles (crater shapes) or with the help of SEM and EDXA which allowed to observe the crack propagation during the earlier stages of erosion and the extent of surface welting by molten silver in the later stages [2, 3]. Other works are quantitative. They concern for instance the mass loss measurement in very different configurations. We can quote for instance the case of an opening contact in DC regime for current intensity in the range 2-35 A [4 - 6] or higher current intensity (250 A) [7], the case of make operations in DC case with I_{make} in the range 200 - 400 A [8, 9], the case of erosion resulting only of the arc action (and not

of the opening phase) for current intensity in the range 200-800 A [10] for an electrode gap in the range 1-10 mm, the case of AC3 or AC4 tests conditions (I_{make} = 600 A and I_{break} = 100 A) [11] and the AC case for arc current in the range 16-100 A [12] or 10-40A [13, 14] up to higher intensity [15] (until 6 kA). Other works concern the volumetric erosion of electrical contacts [16, 17] by the use of a 3D optical profilometer allowing then to quantify the crater dimensions for instance.

B. Objectives

The long term objective of our work is to propose a model of the lifetime of a device such as a contactor. For this purpose, several important preliminary steps are required: a good knowledge of the thermodynamic, thermal and mechanical properties of materials. For instance, experimental works [23, 24] have been conducted concerning the measurement of the properties of Ag-SnO_2 as contact material and their temperature dependence. It is also essential to estimate the power balance at the contacts during the arc in order to assess the metallurgical evolution and wear of the contact pad. This last issue is the main objective of this paper.

There are some modelling works on Ag-MeO type materials, where Me denotes another metal. In most cases, it is assumed to result from evaporation of the electrode material [18 - 21]. In [18], an expression for the power flux density brought by the arc to the electrodes is given. It assumes equipartition between the anode and cathode but no value for the current density or power density is given. In [20], authors consider Ag-CdO electrodes. In [21] they consider pure silver as the electrode material and have taken a maximum power flux density value of 10^{11} W/m² and a current density of the order of 10^{10} A/m².

Concerning the modelling of the lifetime of a contactor, relatively little work has been done. One can mention the work of Yang et al. [22]. They were interested in the evolution of the heating of a relay on a macroscopic scale (temperature of coils and springs) as a function of the number of operations. There are not many works specifically dedicated to the estimation of the power balance in the case of Ag-SnO2 contact electrodes. Two methods previously developed in our laboratory [25] and [26] can be cited.

The first method [25] concerns electric arc with static electrode gaps (in the range 2-10 mm), an arc duration of 20 ms and an arc current intensity equal to 600 A. The second method [26] concerns AC break arc of 300 A rms. In both cases, experimental measurements or observations were compared with results obtained by numerical modelling in order to obtain an estimate of the power balance making experimental results and modelling compatible.

In this work we propose a third indirect method based again on an experimental approach (the measurement of the electrode temperature near the arc impact) and on a modelling step. The objective is again to obtain values on the electrode heating conditions making experiment and model compatible.

The article is divided into different parts:

- The first part is dedicated to the description of the experimental method for measuring the temperature near the area where the opening arc occurs. After a quick bibliographical reminder concerning various methods of temperature measurement implemented in the case of heating of electrodes under the action of an arc, the experimental device (mechanical, optical and electrical) as well as the principle of the method will be described. An example of measurements will then be presented.
- The second part is devoted to the solution of the inverse problem which consists in finding the characteristics of the power flow brought to the electrodes. In this part the method which is based on experimental results and on the use of a 2D numerical thermal model is described with the help of an example. Finally, the results are generalized to various current intensity values for Ag-SnO_2 anodes and cathodes.

II. DESCRIPTION OF THE EXPERIMENTAL METHOD FOR THE MEASUREMENT OF THE ELECTRODE TEMPERATURE NEAR THE ELECTRIC ARC IMPACT.

A. A quick review of different methods used to measure the electrode heating under the electric arc action

Several methods have been proposed to experimentally estimate the electrode temperature resulting from electric arc heating. Among the different possible methods used to measure temperatures, some are based on the use of thermocouples [27]. There are several disadvantages associated with the use of thermocouples for surface temperature measurement. Firstly, the thermocouple will indicate a value related to its own temperature. As a result, the way it is "glued" to the surface can have a significant impact on its own temperature by significantly changing the heating (or cooling) conditions. However, the major drawback is related to the thermal inertia of thermocouples even when very small ones are used (diameter of 100 µm). Thus a phase shift in the temperature rise was estimated to be about a millisecond. If in the case of steady state arcing this is of no consequence, the same cannot be said for non-stationary arcs. Optical measurements were also proposed. Most of them concern arcs in a stationary state in argon between electrodes made of refractory material such as tungsten, thoriated tungsten or hafnium. Among them we can mention Haidar *et al.* [28] who proposed a method to measure the temperature distribution on the edge of a tungsten conical cathode in the case of a stationary arc in argon. To do this they used a spectroscopic method and had to assume that the arc column was immobile and had axial symmetry (axi-symmetry). The measurement is made during the arc period and the assumptions of steady state and axial symmetry then allow using an inverse Abel transform to extract the light emission of the cathode surface from the total radiation and thus to go back to an estimate of the cathode surface temperature. Another reference study comes from Zhou *et al.* [29] who

used single and double wavelength pyrometry. Again, the temperature distribution was measured for tungsten or thoriated tungsten electrodes for stationary arcs and a current intensity of 200 A. They estimated that the arc radiation produced an error in the measurements of less than 2% in the case of a single wavelength pyrometry measurement and 14% in the case of a dual wavelength pyrometry measurement. The emissivity values of tungsten proposed by De Vos [30] were taken in the case of single wavelength pyrometry. The spatial resolution of the results presented is about one measurement point every 50 µm. The fact that they neglected the radiation of the plasma during the arc seems to have been a rather crude hypothesis *a posteriori*, as shown by the work they published afterwards. A third reference work is due to Dabringhausen *et al.* [31] who measured the temperature near the arc root (cathode) in the case of argon arc and tungsten electrodes. For this they used a single wavelength pyrometer. The emissivity values are those of De Vos. The pyrometer detects surface radiation in the range 0.7 - 1.1 µm. The diameter of the sight spot is 0.3 mm. As they work in steady state, the integration time is not specified. Other studies have been carried out in different gases. Peters *et al.* [32] used a dual wavelength pyrometry method. In their case, it is an arc in steady state in oxygen (and in an N_2/O_2 mixture) with hafnium electrodes. To free themselves from the light of the arc, they measured 100 µs after the cut-off and then extrapolated the temperature value at the time of the cut-off. Neither the spatial resolution (size of the measuring spot) nor the integration time of the pyrometer were specified. Teulet *et al.* [33] measured the surface temperature of a steel anode using single or polychromatic pyrometers. The surface area of the spot is about 0.8 mm² and the integration time for measurements is about 0.6 ms.

Other optical measurements were also performed in vacuum. Schellekens *et al.* [34] and Watanabe *et al.* [35] measured, using a fast visible camera and a single wavelength pyrometer, the surface temperature reached at the time of zero crossing of the arc current for 50 Hz arcs of high intensities (several tens of kA) in vacuum and Cu and Cu-Cr electrodes. The integration time was between 0.1 and 1 ms respectively. Little detail is given on the experimental method used. Dullni *et al.* [36] measured with a single wavelength pyrometer the maximum temperature decrease after the vacuum arc cut-off for copper electrodes. Tabulated values for emissivity were taken. No information is given on the spatial and temporal resolution of the measurement and therefore on how the maximum value of the surface temperature is obtained. More recently, Ramanantsoa *et al.* [37] measured with an IR camera the temperature reached on the edges of cylindrical graphite electrodes subjected to an arc of a few tens of A in argon. Quite lately, a method to measure the surface temperature distribution of an electrode a few microseconds after a very fast and controlled extinction of the electrode was proposed [38]. The method used made it possible to measure the surface temperature distribution of copper, carbon or tungsten electrodes [39], [40]. However, such a method requires knowledge of the emissivity of the material in the camera's wavelength range (3.9µm - 5µm). In the case of tungsten, these values were obtained from [30]. In the case of copper, a device was conceived to calibrate the IR camera. It allowed to establish a correspondence between the true temperature (that of the copper specimen) and the camera temperature (calibrated in "black body" temperature). Such a calibration is particularly long and tedious. Indeed, it requires many samples in order to obtain reliable values, and additionally large sample sizes. In the case of Ag-SnO_2, such samples would be particularly expensive and difficult to produce.

B. Description of the method

The proposed approach in the case of Ag-SnO_2 electrodes, was to observe a surface not directly subjected to the arc but close enough to the impacted one, which made necessary to use no massive electrodes. In practice, as we intended to have access to the temperature as close as possible to the arc, thin flat electrodes (a few hundred micrometers thick, in the range 500 µm – 650 µm) were used and the temperature on the side opposite to the electric arc was measured with the help of a IR camera. The employed camera is a Jade MWIR Cedip camera (640 × 512 pixels, spectral range from 3.9 to 5.1 µm). It is calibrated by Cedip system and the correspondence between the measured digital level and the temperature is stored in a calibration curve. The exposure time is controlled and is in the range [10 – 120 µs]. The emissivity problem was answered by spraying the bottom of the electrode with a black heat-resistant paint (Rust-Oleum 750°C). Such a coating has an emissivity greater than 0.9 which leads to an error of less than 3% on the measured temperature. A schematic view of the device is shown in Figure 2. A contact consists of a cylindrical electrode with a curvature radius of about 40 mm on the one hand and a flat electrode of controlled thickness (in the order of a few hundred micrometers) on the other hand. This assembly is mounted on the objective of an IR camera which allows the observation of the lower surface of the flat electrode, thus making it possible to measure its temperature. The objective used gives a spatial resolution such that the size of a pixel is about 40 µm x 40 µm. The upper electrode is mounted on a controllable electrical linear actuator, allowing the contact to be opened. The opening speed is about 300 mm/s. The distance between electrodes is measured using a laser sensor with an accuracy of about 15 µm. On the left side of Figure 2 the device is shown with the contact closed. On the right side it is shown in the presence of an electric arc during the opening phase. A calcium fluoride (CaF_2) window protects the camera lens while allowing the IR wavelengths involved to pass through (transmission coefficient superior to 0.9).

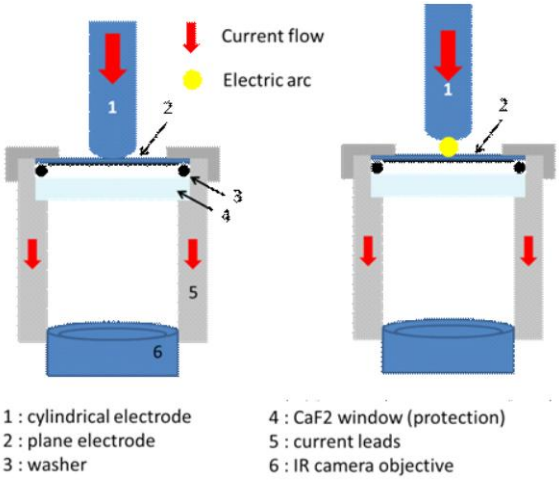

Fig. 2. Schematic representation of the device either when the contact is closed (left) or when the contact is open in the presence of an electric arc (right).

The associated electrical circuit is made up of:

- a power supply (3 car batteries connected in series (36/42 VDC))
- a resistive load allowing the current to be adjusted (up to 1400 A in a near short-circuit configuration)
- an inductive load if necessary
- a safety system (static switching device) allowing the arc to be extinguished if it does not occur naturally.
- In Figure 3 are presented :
- on the right, a schematic view of the electrical circuit,
- on the left, a photo of the device showing the plane and cylindrical electrodes (in the red circle) ; we can see on the plane electrode the traces left by the opening arcs previously made.

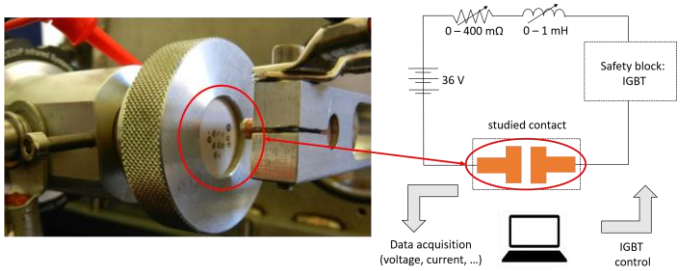

Fig. 3. Schematic view of the electrical circuit and of the device fixed on the camera objective ; the studied contact can be seen in the red circle.

The typical sequence of events occurring for each run is described in Figure 4, which shows the schematic changes in the inter-electrode distance d (in green), contact voltage U_{AC} (in blue) and intensity of the current I_{arc} (in red) flowing through the contact. The whole experience lasts a few milliseconds. A current pulse begins by passing through the initially closed contact (the contact voltage is then a few millivolts). The moments of opening the contact and taking a picture with the IR camera are measured. The exposure time of the camera depends on the temperature range considered, varying from a few microseconds to a few tens of microseconds.

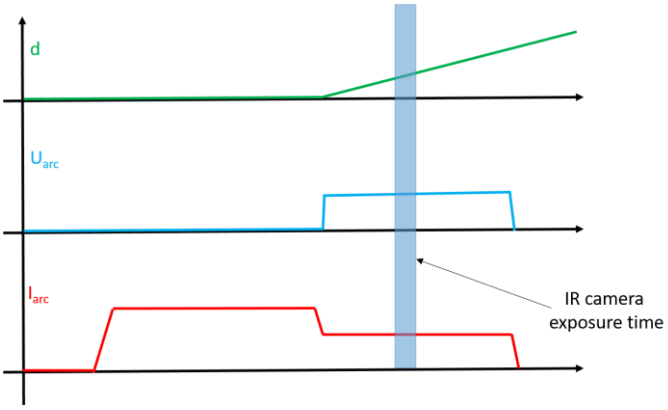

Fig. 4. Schematic representation of the various events as a function of time.

C. *An example of measurement*

Before extracting general results from the various experiments carried out, we will describe in detail an example of a measurement obtained in the case where the flat electrode was a cathode and propose the most complete possible analysis of the obtained results. For the example in question, the current and voltage evolutions are shown in Figure 5. The arc duration is 7.2 ms and the moment of the image capture is 3.3 ms after the ignition of the arc. The resulting 3D thermal mapping is shown in Figure 6. The temperature distribution shown is axially symmetrical. This means that the arc was stationary between its apparition and the image capture. Of course, sometimes, the arc root is mobile on the electrodes and the temperature distribution is no longer axisymmetric. Further on, to solve the inverse problem, it will be necessary to consider only cases where the arc root has been stationary until the temperature measurement. Thus it has been necessary to perform a very large number of arcs in order to select the cases where the arc has remained motionless. Under the same experimental conditions, we made three measurements each time.

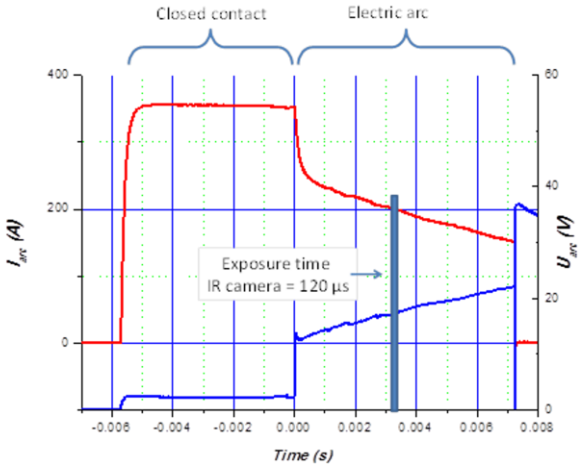

Fig. 5. Evolution of the current intensity (in red) and contact voltage (in blue) for the example considered. The "moment" of the IR image capture is also given.

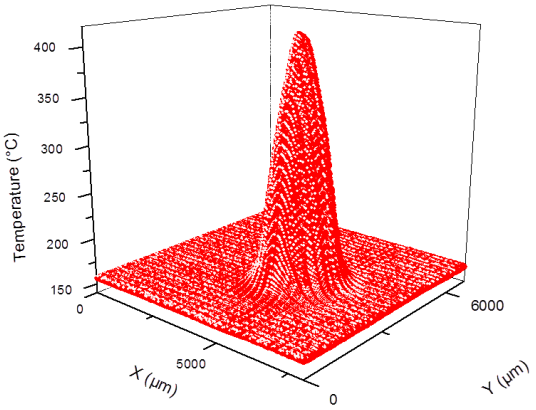

Fig. 6. Thermal mapping obtained for the example considered. Temperature values below 200°C have no physical meaning

It should be noted that temperature values below 200°C have no physical meaning due to the temperature range chosen for the measurement. As a result, the radial extension of the temperature validity area is in the order of 1000 µm. In Figure 7 an example of a temperature profile passing through the maximum temperature (black square dots) is given. A Gaussian fit of this curve, useful in the simulation phase (see next section), was also made and plotted on this figure (pink line).

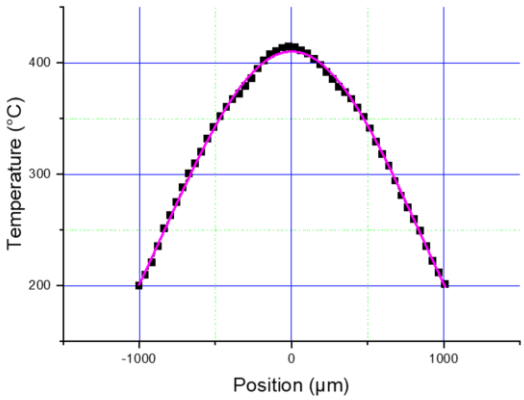

Fig. 7. Temperature profile (square dots) and Gaussian fit curve (in pink).

In the following we will see how, in the case of an immobile arc, information about the power balance can be obtained. This will first be illustrated using the example presented in this section and then generalized to other cases.

III. Solution of the inverse problem: estimation of the power balance at the electrode.

A. A macroscopic approach for the power balance at the electrode

To describe the power balance at the electrode surface, a macroscopic point of view is adopted. We have used the formalism already chosen by several authors [41,42] which introduces an apparent arc root and an effective arc spot current density. This formalism synthesizes the different physical phenomena occurring at the microscopic scale that contribute to the heating of the electrode (ion bombardment, electron emission, neutral bombardment, radiation…) and the power flow is characterized by two quantities: the power denoted P (in W) and the surface power density denoted Q (in W/m²) brought by the arc to the electrodes. They are given in the following forms:

$$P(t) = I_{arc}(t) \times V_{eq}(t) \qquad (1)$$

$$Q(r,t) = J(r,t) \times V_{eq}(t) \qquad (2)$$

with I_{arc} the intensity of the arc current, V_{eq} an equivalent voltage and J the "apparent" current density which can be a function of the position. The aim of the approach will therefore be to estimate the two parameters V_{eq} and J or Q. V_{eq} *a priori* does not represent the classic voltage drop near the electrodes. As an example, we remind that for Ag-SnO_2 electrodes in air, the sum of the anode and cathode drop (V_A + V_C) is 15 V [43]. In the following we will note P_C and Q_C (respectively P_A and Q_A) the power and the power flux density supplied by the arc to the cathode (respectively to the anode),

and $J_C(r)$ (respectively $J_A(r)$) the apparent current density in the cathode root (respectively the anode root). A first simple hypothesis is to consider that the current density in the arc root is uniform. Indeed, in the field of modeling, we can find works proposing a uniform current density or a current density depending on the radial coordinate. From an experimental point of view, many works [44 - 50] have been done to determine the current density at the cathodic arc root and many values have been proposed for "cold" cathodes (Cu, Ag, Ni, ...) obtained from either the observation of the tracks left by the root of the arc, or the observation of the of the luminous zone on the surface of the cathode, or the spectroscopic study (Zeeman effect) or the use of coils in the cathode or the measurement of the force exerted by the arc on the electrode. In all cases, the values obtained correspond to spatial average values, which means that a uniform current density is considered.

In these conditions:

$$J(r) = J_0 \; and \; Q(r) = Q_0 \qquad (3)$$

with:

$$Q_0 = V_{eq} \times J_0 \qquad (4)$$

Obviously we have :

$$I_{arc}(t) = \pi \times a^2(t) \times J_0 \quad (5)$$

where $a(t)$ is the arc root radius.

B. *Description of the numerical modelling.*

The geometry taken into account in our model is given in Figure 8. It is a flat Ag-SnO_2 electrode with a radius (denoted R) of 12.5 mm and a thickness (which is measured for each test) in the range 500-650 µm (obviously for readability reasons, the figure is not to scale). A 2D numerical model of the electrode heating is used. It has been already described in [51].

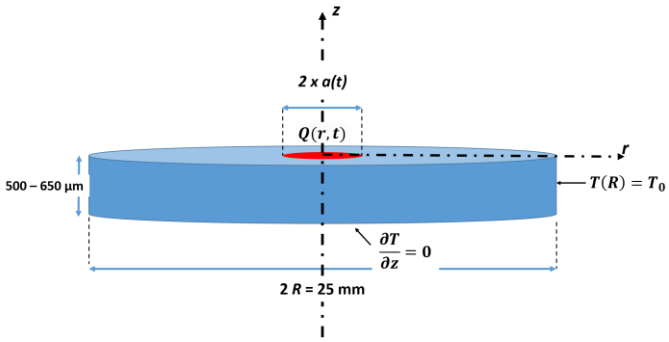

Fig. 8. Schematic view of the axisymmetric geometry and boundary conditions considered for the model.

The heat diffusion in the electrode is described by the equation $\rho C_p \frac{\partial T}{\partial t} = \vec{\nabla}.\left(k\vec{\nabla}T\right) + P_J$ (6)where ρ is the density, C_p the specific heat, T the temperature, t the time, k the thermal conductivity and P_J the Joule power density. As usual, for such electric arc P_J is negligible. It has been shown that the Joule power is no longer negligible at current densities above 10^{11} A/m² [52].

Concerning the boundary conditions, the upper surface ($z = 0$) of the contact pad is heated by the flux characterized by the power and the power flux density.

$$-k.\frac{\partial T}{\partial z} = Q_0 \;\; if \; r \leq a(t) \; and \; 0 \; if \; r > \; a(t)$$

The arc root is supposed to be motionless. The side edges ($r = R$) of the pad are sufficiently far from the arc root and the duration of the arc is short enough to consider their temperature constant during the arc (equal to the ambient temperature T_0 : $\forall z, \forall t, T(R) = T_0$). Convection and radiation cooling of the electrode have been neglected, so that the heat flux on the underside is considered to be zero. This is justified because of the short arc duration. Solving the heat equation during heating thus gives the evolution of the spatial temperature distribution. An enthalpic method was used to deal with the problem of phase change. The specific heat, mass density and thermal conductivity values are taken from [23] for the solid state material. They were determined experimentally. For the liquid state, they come from the model proposed in [53].

Heating is therefore only the result of the application of power flows modelling the heating by the root of the arc. In this respect, the quantities V_{eq} and Q_0 were considered constant during heating.

C. *Application of the method to an example.*

The objective is then to find the V_{eq} and Q_0 values that will allow us to get "as close as possible" to the experimental temperature profile. For several values of V_{eq}, we have varied the value of Q_0. The results for the deviation value between calculated and experimental curves have then been calculated as a function of Q_0 for the various V_{eq}. The uncertainty on the value of the measured temperature is of the order of 2.5% (due to the emissivity value of the heat-resistant paint). As a criterion of compatibility between experience and calculation, the value of the maximum difference between the calculated and measured curves should be less than or equal to 5% of the maximum heating (twice the inaccuracy due to the paint). By way of illustration, for the case of figures 6 and 7, the maximum temperature rise is 425°C and we have therefore retained the couples (V_{eq} ,Q_0) which led to a difference between the curves of less than 21°C. We have plotted in figure 9 the maximum temperature difference reached (denoted ΔT_{max}) as a function of the value of Q_0 for two values of V_{eq} (5 V and 6 V). We can see that a compatibility zone exists for V_{eq} = 5 V whereas none is possible for V_{eq} = 6 V.

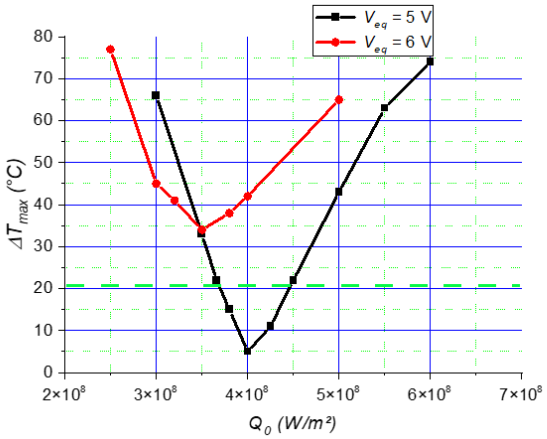

Fig. 9. Value of ΔT_{max} as a function of Q_0 for two values of V_{eq}. The line marking 5% of the temperature rise is specified in green.

Figure 10 shows a summary of the calculations by determining an area in the axes V_{eq}, Q_0 in which the measured and calculated temperature profiles check the criterion on T_{max}.
By way of comment, a complementary angle can be mentioned. We have indeed other information at our disposal: for example the possibility to observe the crater left by the arc with a 3D optical profilometer, which allows to investigate another criterion based on topographical data. Figure 11 gives a surface profile of this crater along a diameter. The minimum melted depth is of the order of 35-40 µm and the minimum melted diameter is of the order of 760 - 780 µm. Calculations carried out for couples (V_{eq} , Q_0) leading to profiles compatible with the experiment led to melted depths always greater than 44 µm and melted diameters greater than 800 µm. In this case the two criteria (temperature profiles and crater dimensions) are met.

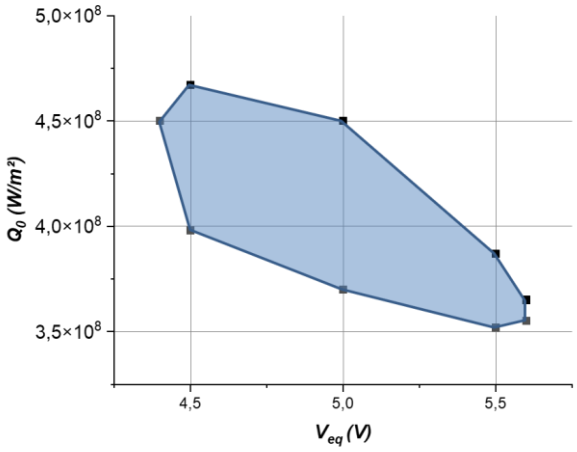

Fig. 10. Zone of compatibility between experiment and modelling for the determination of Q_0 and V_{eq} in the case presented as an example.

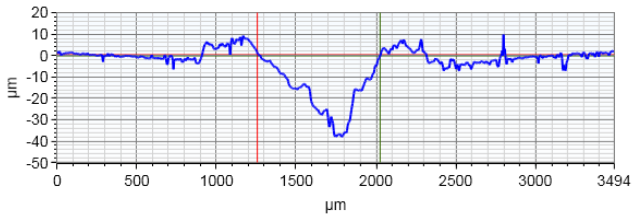

Fig. 11. Observation of a diametric profile of the crater left by the arc with an optical profilometer. The minimum molten diameter is of the order of 760 - 780 µm. The minimum melted depth is of the order of 35 - 40 µm.

D. Example of results.

Several experimental tests have been carried out and the reverse problem has been solved. In this section we present some examples of the power balance obtained for three different values of the arc current intensity: 80, 125 and 200 A in the case of anode and cathode. Thus, Figures 12 and 13 give the compatibility zones for an anode and a cathode, respectively, for the three values of the arc current intensity. With the same duration, the erosion increases due to the increase of the power supplied to the electrodes. There is no physical reason for the fact that V_{eq} for I_{arc} = 200 A, in the case of an anode, is lower than V_{eq} for I_{arc} = 125 A. However, it should be noted that in our case this is a single example and that a statistical study would be necessary. On this subject, in the case of copper electrodes, some authors have proposed an estimate of V_{eq} as a function of I_{arc}. It was observed [54] that the mean value of V_{eq} seemed to depend little on I_{arc} in the range 150 A - 500 A and that a very strong dispersion in the results appeared (for I_{arc} = 280 A V_{eq} is in the range 4 -11 V). It is then possible to have V_{eq} of the order of 9V for 125 A, 5V for 280 A and 8 for 500 A. Other authors [55], for lower currents, have estimated the power supplied to the electrodes as a function of the current for different inter-electrode distances. By introducing the notion of V_{eq} at constant inter-electrode d, we can estimate the variation of V_{eq} with current (in the range [1-30] A). It can be seen that the variation of V_{eq} is a decreasing function of I_{arc}.

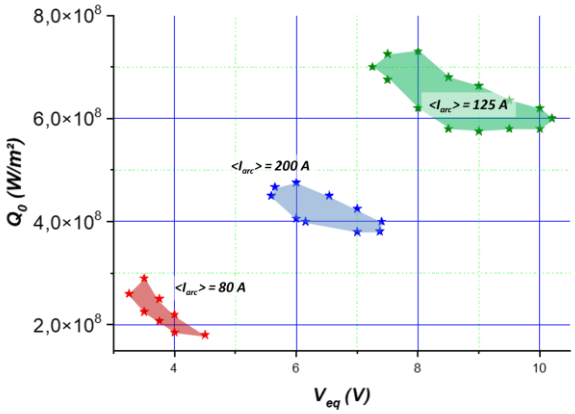

Fig. 12. Synthesis of the areas of compatibility between experiment and modelling in the case of an anode for various average values of the arc current intensity.

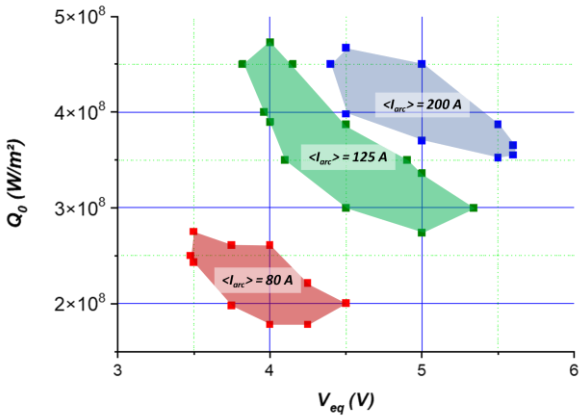

Fig. 13. Synthesis of the areas of compatibility between experiment and modelling in the case of a cathode for various average values of the arc current intensity.

Moreover, the fact that V_{eq} is not an increasing function of I_{arc} does not mean that the power input is not increasing. This can be seen in Figure 14 where we have plotted the power versus the arc current.

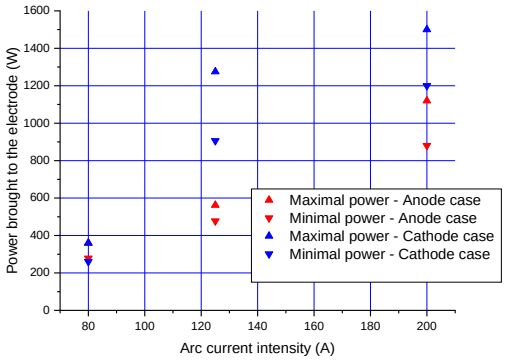

Fig. 14. Power brought by the electric arc to the electrode as a function of the current intensity values: 80, 125 and 200 A

IV. Conclusions

We have presented a simple method allowing to obtain information concerning the characteristics of the power flux brought by an electric arc to an Ag-SnO_2 electrode (anode and cathode) in the case of an arc of short duration and short electrode gap. This method is based on the measurement of the temperature distribution close to the arc root and the use of a model of the thermal phenomena occurring in the heated electrode. For a given electrode it is possible to find a zone of values for the couple power and surface power density compatible with the experimental observations. We have obtained an estimation of the 'most compatible' values for the power and surface power density. It has been found for Ag-SnO_2 anodes and cathodes that:

$$3{,}7\ V < V_{eqA} < 10{,}2\ V$$
$$3{,}5\ V < V_{eqC} < 5.6\ V$$
$$1{,}9 \times 10^8 W.m^{-2} < Q_{0A} < 7{,}2 \times 10^8 W.m^{-2}$$
$$1{,}8 \times 10^8 W.m^{-2} < Q_{0C} < 4{,}8 \times 10^8 W.m^{-2}$$

In a future article, we will present a new method to obtain values for V_{eq} and Q_0. The results obtained by each method will be compared.

This work has benefited from the financial support of the LabeX LaSIPS (ANR-10-LABX-0040-LaSIPS) managed by the French National Research Agency under the "Investissements d'avenir" program (n°ANR-11-IDEX-0003-02).

References

[1] A. Fouque et al., "Observation of metallurgical changes induced by an electric arc on Ag-SnO_2-CuO electrodes", in Proc. 65th IEEE Holm Conference on Electrical Contacts, pp..239-244, 2019.

[2] M. Hasegawa, K. Takahashi, "Observation of changes of contact surface profiles of Ag and AgSnO2 contacts during switching operations with an optical cross-section method", in Proc. 58th IEEE Holm Conference on Electrical Contacts, pp 280-286, 2012.

[3] M. Hasegawa et al., « Comparison of transfer and erosion shapes on Ag and AgSnO2 contacts caused by break arc discharges in a DC inductive load circuit", in Proc. 59th Holm Conference on Electrical Contacts, pp. 288-294, 2013.

[4] N. Ben Jemaa *et al.*, « Break Arc Duration an Contact Erosion in Automotive Application », *IEEE Transactions on Components, Packaging, and Manufacturing Technology*: Part A (Volume: 19 , Issue: 1 , Mar 1996), pp. 82-86.

[5] J. Swingler *et al.*, "The evolution of contact erosion during an opening operation at 42V", in Proc. 51th IEEE Holm Conference on Electrical Contacts, pp. 346-351, 2005, DOI: 10.1109/HOLM.2005.1518268.

[6] J. Swingler and J.W. McBride, "The erosion and arc characteristics of Ag/CdO and Ag/SnO2 contact materials under DC break conditions", *IEEE Transactions on Components, Packaging, and Manufacturing Technology: Part A*, vol. 19, Issue: 3, Sep 1996, pp. 404 – 415, DOI: 10.1109/95.536842.

[7] V. Berhens *et al.*, "Influence of contact material on the performance of a DC contactor", in Proc. 43th IEEE Holm Conference on Electrical Contacts, pp. 97-103, 1997, DOI: 10.1109/HOLM.1997.638001.

[8] E. Hetzmannseder and W. Rieder, « Make-and-break erosion of Ag/MeO contact materials", in Proc. 41th IEEE Holm Conference on Electrical Contacts, pp. 365-372, 1995, DOI: 10.1109/HOLM.1995.482893.

[9] P. Braumann *et al.*, « Optimization of the break-arc erosion performance of contact materials in switching devices", In Proc. 44th IEEE Holm Conference on Electrical Contacts, pp. 269-275, 1998, DOI: 10.1109/HOLM.1998.722455.

[10] A. M. Gouega *et al.*, « Study of the electrode gap influence on electrode erosion under the action of an electric arc », *Eur. Phys. J. AP*, 11, 111-122, 2000

[11] H. Manhart and W. Rieder, "Erosion behavior and 'erodibility' of Ag/CdO and Ag/SnO2 contacts under AC 3 and AC 4 test conditions", *IEEE Transactions on Components, Hybrids, and Manufacturing Technology*, vol. 13, Issue: 1 , Mar 1990, pp. 56-64, DOI: 10.1109/33.52878.

[12] R. Mingzhe and W. Qiping, "Effects of additives on the AgSnO2 contacts erosion behavior", in Proc. 39th IEEE Holm Conference on Electrical Contacts, pp. 33-36, 1993, DOI: 10.1109/HOLM.1993.489657.

[13] J. Swingler, J.W. McBride, "The net zero mass loss phenomenon on opening switching contacts with AC loading", *IEEE Transactions on Components and Packaging Technologies*, vol. 22 , Issue: 1 , pp.27-37, 1999, DOI: 10.1109/6144.759350.

[14] Wang Kejian, Wang Qiping, "Erosion of silver-base material contacts by breaking arcs», in Proc. 36th IEEE Holm Conference on Electrical Contacts, and the 15th International Conference on Electrical Contacts, 1990, pp. 44-48, DOI: 10.1109/HOLM.1990.112993.

[15] J. Shea "High Current AC Break Arc Contact Erosion", in Proc. 54th IEEE Holm Conference on Electrical Contacts, pp. xxiv-xliv, 2008.
[16] D. Zhang *et al.*, « Evaluation of the volumetric erosion of spherical electrical contacts using the defect removal method", *IEEE Transactions on Components and Packaging Technologies*, vol. 29, Issue: 4, pp. 711-717, 2006, DOI: 10.1109/TCAPT.2006.880523.
[17] J.W. McBride *et al.*, "On the evaluation of low level contact erosion", in Proc. 50th IEEE Holm Conference on Electrical Contacts and the 22nd International Conference on Electrical Contacts Electrical Contacts, pp. 370-377, 2004, DOI: 10.1109/HOLM.2004.1353143.
[18] Ming Sun *et al.*, "The model of interaction between arc and AgMeO contact materials", IEEE Transactions on Components, Packaging, and Manufacturing Technology: Part A, vol. 17, Issue: 3, pp. 490-494, 1994, DOI: 10.1109/95.311761.
[19] J. Swingler, J.W. McBride, "Modelling of energy transport in arcing electrical contacts to determine mass transfer", in Proc. 42th IEEE Holm Conference on Electrical Contacts. And of 18th International Conference on Electrical Contacts, pp. 105-114, 1996, DOI: 10.1109/HOLM.1996.557186.
[20] F. Pons, M. Cherkaoui "An Electrical Arc Erosion Model Valid for High Current: Vaporization and Splash Erosion", in Proc. 54th IEEE Holm Conference on Electrical Contacts, pp. 9-14, 2008, DOI: 10.1109/HOLM.2008.ECP.15.
[21] X. Zhou *et al.*, "Evaporation Erosion of Contacts Under Static Arc by Gas Dynamics and Molten Pool Simulation", *IEEE Transactions on Plasma Science*, vol. 43, Issue: 12, pp. 4149 – 4160, 2015, DOI: 10.1109/TPS.2015.2497720.
[22] W. Yang *et al.* "Simulation and Experimental Study of Thermal Effects on Composite Contacts in Electrical Life Cycle Tests of DC Relays", *IEEE Transactions on Components, Packaging and Manufacturing Technology*, vol. 5, Issue: 6, pp. 745 – 754, 2015, DOI: 10.1109/TCPMT.2015.2437363.
[23] A. Fuentes, « Étude expérimentale et numérique de l'assemblage du matériau de contact Ag-SnO2 (88/12) par procédé résistif », *Ph. D Dissertation*, Université Européenne de Bretagne, France, 2010.
[24] A. Fouque, « Contribution à l'étude du couplage thermique-mécanique-électrique dans les contacts électriques : application à l'élaboration d'un modèle de durée de vie d'un contacteur », *Ph. D Dissertation*, Université Paris Saclay, France, 2020.
[25] Ph. Teste *et al.*, « Détermination des caractéristiques du flux de puissance apporté à des électrodes en AgSnO2 par un arc non stationnaire dans l'air », in Proc. 13th Colloque sur les Arcs Electriques et Workshop Arcs et Contacts Electriques (CAE XIII ACE 2017), Mar 2017, Nancy, France. ⟨hal-01481584⟩
[26] A. Fouque *et al.*, « Estimation of the power flux supplied by an electric arc to Ag-SnO2 electrodes based on cross-section observations of the melted zone", *European Physical Journal: Applied Physics*, 89, 20901, (2020). DOI: 10.1051/epjap/2020190222
[27] F. Uhlig, "Contribution à l'etude des effets directs du foudroiement sur les materiaux structuraux constituant un aeronef », *Ph D Dissert*ation, Universiét Paris , France, 1998.
[28] J Haidar and A J D Farmer « Surface temperature measurements for tungsten-based cathodes of high-current free-burning arcs", *Journal of Physics D: Applied Physics*, vol. 28, n° 10, pp. 2089-2094, 1995.
[29] Zhou *et al.*, "Temperature measurement and metallurgical study of cathodes in DC arcs", in Proc 41th IEEE Holm Conference on Electrical Contacts, pp. 219-231, 1995, DOI: 10.1109/HOLM.1995.482874.
[30] J. C. De Vos « A new determination of the emissivity of tungsten ribbon », *Physica*, pp. 690-714, 1954
[31] L. Dabringhausen *et al.*, "Determination of HID electrode falls in a model lamp I: Pyrometric measurements", *J. Phys. D: Appl. Phys*, vol. 35, pp. 1621-1630, 2002.
[32] J. Peters *et al.*, "Erosion mechanisms of hafnium cathodes at high current", *J. Phys. D: Appl. Phys.*, vol. 38, n° 11, pp. 1781-1794,, 2005, doi.org/10.1088/0022-3727/38/11/019.
[33] Ph. Teulet *et al.*, « Experimental study of an oxygen plasma cutting torch: II. Arc–material interaction, energy transfer and anode attachment », *J. Phys. D:Appl. Phys*, 2006, 39, pp. 1557-1573, https://doi.org/10.1088/0022-3727/39/8/015
[34] H. Schellekens, M.B. Schulman, "Contact temperature and erosion in high-current diffuse vacuum arcs on axial magnetic field contacts", *IEEE Transactions on Plasma Science*, vol. 29, Issue: 3, pp. 452-461, 2001, DOI: 10.1109/27.928943.
[35] K. Watanabe *et al.*, « Technological progress of axial magnetic field vacuum interrupters", *IEEE Trans. Plasma Science*, 25, pp. 609-616, 1997, DOI: 10.1109/27.640673
[36] E. Dullni *et al.*, "Electrical and pyrometric measurements of the decay of the anode temperature after interruption of high-current vacuum arcs and comparison with computations", *IEEE Transactions on Plasma Science*, vol. 17, Issue: 5, pp. 644 – 648, 1989, DOI: 10.1109/27.41173.
[37] R Ramanantsoa *et al.*, "Experimental quantification of the transient heat flux transferred to the electrodes in a carbon nanotubes synthesis reactor", *J. Phys.: Conf. Ser*.275 012002, 2011, doi:10.1088/1742- 6596/275/1/012002
[38] R. Landfried, " Contribution à l'étude de la transition décharge luminescente / arc électrique dans l'air et dans l'argon au voisinage de la pression atmosphérique. », *Ph D Dissertation*, Supelec, France, 2011.
[39] R. Landfried *et al.*, « Temperature Measurement of Copper Contact Surfaces", in Proc. 56th IEEE Holm Conference on Electrical Contacts, pp. 148-152, 2010, DOI: 10.1109/HOLM.2010.5619548 .
[40] R. Landfried *et al.*, "Temperature Measurement of Tungsten Electrode Surface at Electric Arc Extinction in Air–Power Flux Estimation", *IEEE Transactions on Components, Packaging and Manufacturing Technology*, vol. 4, Issu: 10, pp. 1606 – 1612, 2014, DOI: 10.1109/TCPMT.2014.2343792.
[41] A. Marotta *et al.*, "Heat Transfer and Cold Cathode Erosion in Electric Arc Heaters", IEEE Transactions on Plasma Science, vol. 25, n° 5, pp. 905-912, 1997.
[42] A. Lefort *et al.*, "Determination of the power lost by conduction into the cathode at low current arc", *J. Phys. D : Appl. Phys.*, 28, pp. 1883-1887, 1995.
[43] A.M. Gouega, *et al.* "Study of the electrode gap influence on electrode erosion under the action of an electric arc" Eur. Phys. J. AP 11, 111–122 (2000)
[44] C C lsanger and P.E. Secker, "Arc cathode current density measurements", *J. Phys. D: Appl. Phys.* 4, 1940 (1971).
[45] K.P. Nachtigall and J. Mentel, "Measurement of arc spot formation delay times at cold cathodes in air", *IEEE Trans. Plasma Sci.* 19, 942 (1991).
[46] A.E. Guile, « Arc-electrode phenomena », *Proc. I.E.E.* 118, 1131 (1971)
[47] R.N. Szente, M.G. Drouet, R.J. Munz, "Current distribution of an electric arc at the surface of plasma torch electrodes", *Appl. J. Phys.* 69, 1263 (1991).
[48] K.C. Tsu, K. Etemadi, E. Pfender, "Study of the free-burning high-intensity argon arc", *Appl. J. Phys.* 54, 1293 (1983).
[49] N. Vogel and B. Juttner, "Measurements of the current density in arc cathode spots from the Zeeman splitting of emission lines", *J. Phys. D: Appl. Phys.* 24, 922 (1991).
[50] J. Devautour, « Contribution à l'étude des interactions arc-electrodes. Influence de la structure métallurgique sur les mécanismes d'érosion des appareils de coupure », Ph.D. thesis, Paris 6 University, France,1992.
[51] J. P. Chabrerie, J. Devautour, and Ph. Teste "A Numerical Model for Thermal Processes in an Electrode Submitted to an Arc in Air and Its Experimental Verification" IEEE Transactions On Components, Hybrids, And Manufacturing Technology, Vol. 16, No. 4, June 1993.
[52] Z. J. He and R. Haug "Cathode spot initiation in different external conditions" 1997 J. Phys. D: Appl. Phys. 26 603–13.
[53] A. Bonhomme, PhD thesis, Ecole nationale supérieure des Mines de Nancy (2005).
[54] A. M. Essiptchouk et al., « Magnetic field effect on the volt equivalent of arc spot heat flux », Contrib. Plasma Phys. 45, n°7, 522-530 , 2005, DOI 10.1002/ctpp. 200510058
[55] W. Rieder, « Leistungsbilanz des Elektroden und Charakteristiken frei brennender Niederstrombögen »,Zeitschrift für Physik, Bd. 146, S. 629-643, 1956